Journal of Electrical Engineering and Renewable Energies Development (JEERED)
Vol. N°: 1, Issue N°: 2, pp. 67-73, 2025.

Digital Fuzzy Logic and Dahlin Control Design for a DC-DC Boost Converter

Ghrissi TAHRI[1], Fatima TAHRI[2], and Ali TAHRI[3]

[(1)]Institute of Science and Applied Technology (ISTA), University of Oran 1, Ahmed Ben Bella, B.P. 1524, El M'Naouer, Oran 31000, Algeria

[(2)]Laboratoire de Développement des Réseaux Electriques Intelligents (LDREI), Ecole Supérieure en Génie Electrique et Energétique d'Oran (ESGEE), Chemin Vicinal N 9, Oran 31000, Algérie

[(3)]Electrical Engineering Laboratory, Electrical Engineering Faculty, University of Science and Technology of Oran, Mohamed Boudiaf USTO-MB, BP 1505 El M'naouer, Oran,31000, Algeria

Email of the corresponding author: tahri.ghrissi@univ-oran1.dz , ghrissi.tahri@univ-usto.dz

***Abstract*—**This article presents an innovative methodology for digital control rules applicable to a DC-DC boost converter (BC). The State-Space Averaged (SSA) approach was used to develop the converter mathematical model, a crucial step in the control design of this study. The voltage control mode (VCM) for the continuous conduction mode (CCM) was implemented with utmost care and precision. The two discrete fuzzy logic controllers (FLC) and Dahlin were meticulously and rigorously synthesized, ensuring the method's robustness. An analysis of the amplitude variations in input voltage and load is also conducted to compare these two digital controllers. The method's efficacy is not just claimed but thoroughly validated. The simulation results, acquired via the SimPowerSystems MATLAB, are presented and discussed, providing concrete evidence of the control method's effectiveness.

Keywords*—DC-DC boost converter, SSA, FLC, Dahlin.*

I. INTRODUCTION (*HEADING 1*)

A power electronics system employs power semiconductor devices to transform electrical energy from one form to another and deliver it to a load. Since the 1970s, researchers have been conducting studies and developing various types of DC-DC converter circuits. One such converter is capable of either boosting or bucking the output voltage. The DC-DC BC is a prevalent design that employs a switch in parallel with the supply voltage to produce an output voltage exceeding the input voltage [1].

The continuous conduction mode (CCM) encompasses two topologies, while the discontinuous conduction mode (DCM) requires an additional configuration, resulting in three distinct topologies [2]. In every configuration, the system can be described by linear state equations. The switching between topologies will depend on the system output, adding complexity to the study. This converter is known for its highly dynamic, non-linear components due to power-switching devices. The mean state space technique is widely utilized for modeling the DC-DC BC.

The DC-DC BC model is typically nonlinear due to its multiplicative elements, including state variables and the duty cycle [3]. This nonlinearity masks information about the system's rapid dynamics, making fast instabilities such as sub-harmonic oscillations challenging to detect and analyze [4].

Therefore, this paper presents a mathematical model for the DC-DC BC's CCM mode, utilizing the SSA approach as its contribution.

This study compares FLC and Dahlin digital controllers. One advantage of utilizing fuzzy logic to

represent human raisoning is the ability to express rules in simple language, allowing for greater flexibility in reasoning to accommodate imprecision and uncertainty. In contrast, the Dahlin digital controller produces the system's output in exponential format [5].

The reference voltage tracking tests involved critical changes in input voltage levels and loads of the DC-DC BC. These tests were conducted using MATLAB/Simulink to validate the effectiveness and stability of the digital controllers proposed in this study.

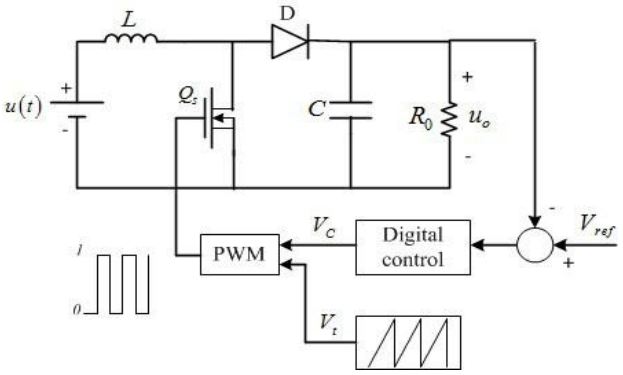

Fig. 1. DC-DC BC in association with the digital controller.

II. Modeling of DC-DC BC using the SAA method:

The initial step is to identify the equations that govern the two topologies, which are the switch-on and switch-off Qs MOSFETs. The block diagram in Fig. 1 illustrates the DC-DC BC in association with the digital controller.

A. *Switch-off of the MOSFET:*

The switch Qs is closed, and the diode is blocked. The state variables are the inductor current and the capacitor voltage, denoted respectively by $i_L(t)$ and $v_C(t)$, whose state vector is defined by $x(t)' = \left[i_L(t) \quad v_C(t) \right]'$.

Using Kirchhoff's laws and rearranging the terms of the differential equations, the state-space model of this mode is defined as follows:

$$\begin{aligned} \dot{x}(t) &= M_1 x(t) + N_1 u(t) \\ y(t) &= O_1 x(t) \end{aligned} \tag{1}$$

Such as:

$$M_1 = \begin{bmatrix} 0 & 0 \\ 0 & -\dfrac{1}{C R_0} \end{bmatrix}; \quad N_1 = \begin{bmatrix} \dfrac{1}{L} \\ 0 \end{bmatrix}; \quad O_1 = \begin{bmatrix} 0 & -1 \end{bmatrix} \tag{2}$$

B. *Switch-on of the MOSFET:*

The switch Qs is opened, and the diode is on. By using Kirchhoff's laws and rearranging the terms of the differential equations, the state-space model of this mode is defined as follows:

$$\begin{aligned} \dot{x}(t) &= M_2 x(t) + N_2 u(t) \\ y(t) &= O_2 x(t) \end{aligned} \tag{3}$$

Such as:

$$M_2 = \begin{bmatrix} 0 & -\dfrac{1}{L} \\ \dfrac{1}{C} & -\dfrac{1}{C R_0} \end{bmatrix}; \quad N_2 = \begin{bmatrix} \dfrac{1}{L} \\ 0 \end{bmatrix}; \quad O_2 = \begin{bmatrix} 0 & 1 \end{bmatrix} \tag{4}$$

C. *Model average for DC-DC BC:*

The linearization strategy of the SSA can establish the combination between the two state spaces. There are only two duty ratios of the switching period to consider for this DC-DC BC: the ratio for when the system is switched on and when the system is switched off. The average matrices can be expressed as:

$$M = \left[M_1 d + M_2 (1-d) \right] = \begin{bmatrix} 0 & -\dfrac{(1-d)}{L} \\ \dfrac{(1-d)}{C} & -\dfrac{1}{C R_0} \end{bmatrix} \tag{5}$$

$$N = \left[N_1 d + N_2 (1-d) \right] = \begin{bmatrix} \dfrac{1}{L} \\ 0 \end{bmatrix} \tag{6}$$

III. Linearization of the DC-DC BC model using the SSA method's small signal approach:

Transfer functions for control analysis are derived from the SSA model's state equations, which represent a linear approximation to the system. Small-signal analysis is the technique utilized here.

Small perturbed quantities are utilized in place of state variables and control parameters in small-signal analysis [6]. The SSA model's previous state equations are transformed into two modes of equation expressed as follows:

- DC-mode equations model:

$$\left[M_1 d + M_2 (1-d) \right] x_0 + \left[N_1 d + N_2 (1-d) \right] u_0 = 0 \tag{7}$$

- AC-mode equations model:

$$\begin{aligned} \dot{\hat{x}}(t) = &\left[M_1 d + M_2 (1-d) \right] \hat{x}(t) + \left[N_1 d + N_2 (1-d) \right] \hat{u}(t) \\ &+ \left[(M_1 - M_2) x_0 + (N_1 - N_2) u_0 \right] \hat{d}(t) \end{aligned} \tag{8}$$

The AC-mode equations can be written in matrix form as follows:

$$\begin{bmatrix} \dot{\hat{i}}_L(t) \\ \dot{\hat{v}}_C(t) \end{bmatrix} = \begin{bmatrix} 0 & -\frac{(1-d)}{L} \\ \frac{(1-d)}{C} & -\frac{1}{CR_0} \end{bmatrix} \begin{bmatrix} \hat{i}_L(t) \\ v_C(t) \end{bmatrix} + \begin{bmatrix} \frac{1}{L} \\ 0 \end{bmatrix} \hat{u}(t) + \begin{bmatrix} 0 & \frac{1}{L} \\ -\frac{1}{C} & 0 \end{bmatrix} \begin{bmatrix} I_L \\ V_C \end{bmatrix} \hat{d}(t) \quad (9)$$

To deduce the steady-state solutions I_L and V_C, it's necessary to solve the continuous-mode system given by Eq. (7).

$$I_L = \frac{u_0}{R_0 (1-d)^2} \quad (10)$$

$$V_C = \frac{u_0}{(1-d)} \quad (11)$$

The ratio of the load terminal voltage $\hat{V}_C(s)$ to the duty cycle $\hat{d}(s)$ forms the transfer function that can be determined as follows:

$$\frac{\hat{V}_C(s)}{\hat{d}(s)} = \frac{\frac{u_0}{LC}\left(\frac{L}{R_0(1-d)^2}s+1\right)}{s^2 + \frac{1}{R_0 C}s + \frac{(1-d)^2}{LC}} \quad (12)$$

IV. Discrete Fuzzy Logic Controller Design :

The discrete fuzzy logic controller's input is specifically associated with the error and its variation, while the output corresponds to the duty cycle's variation as shown in the Fig. 2.
The discrete FLC consists of 3 blocks which are:

A. Fuzzification:

In this step, the input and output values are converted into fuzzy subsets in the form of membership functions [7]. These membership functions are identical for the input and its variation as well as for the output. They consist of seven functions: five triangular centered around zero and two trapezoidal at the extremity, limited by an interval of [-1, 1], as shown in Figure (3).

B. Fuzzy Inference Rules:

The fuzzy inference mechanism determines the outputs corresponding to fuzzy inputs using fuzzy logic reasoning [8]. The fuzzy rule base consists of the IF-THEN syntax, which depicts the fuzzy rules of the discrete FLC (Figure. 4).

C. Defuzzification:

Is the final step in an operational discrete FLC. Defuzzification aims to merge these commands and transform the resulting parameters into numerical data [9], [10].

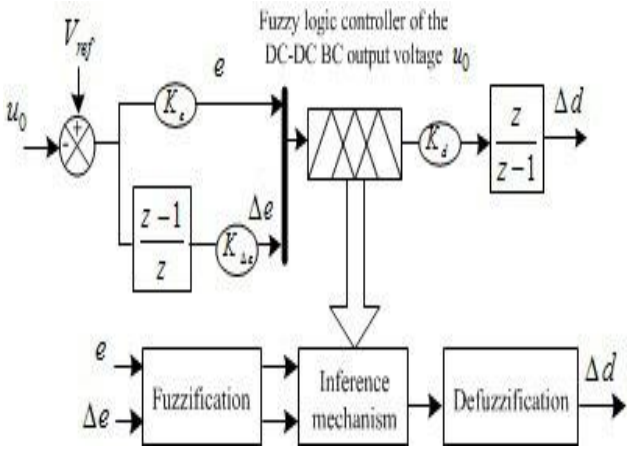

Fig. 2. FLC Process block diagram for DC-DC BC output voltage control.

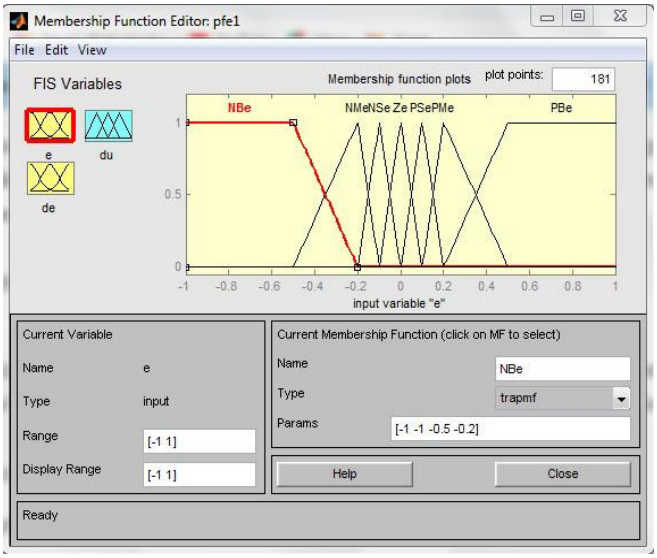

Fig. 3. Discrete FLC membership functions of error and its variation and control.

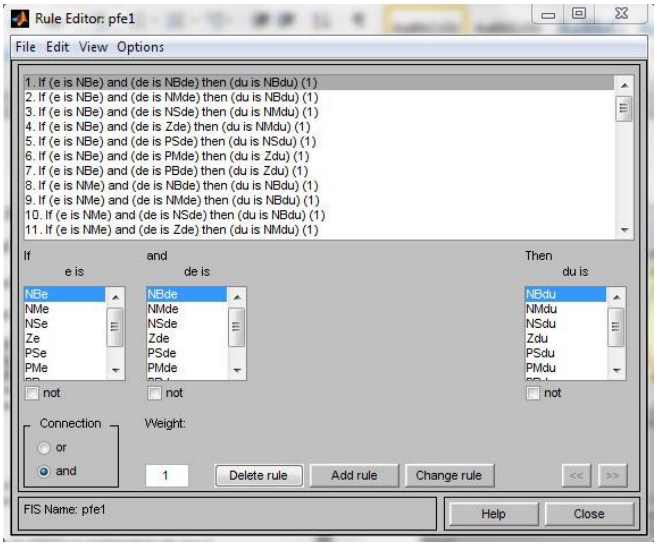

Fig 4. Discrete FLC fuzzy inference rules.

V. Design of the Dahlin Digital Controller:

The Dahlin digital controller renders the system response as exponential [11]. The system response in the Laplace domain is that of the following formula:

$$Y(s) = \frac{1}{s}\frac{e^{-\alpha s}}{1+s\lambda} \tag{13}$$

Where α is the delay, and λ is the time constant. The delay is set as $\alpha = K\,T$ and the Z-transform of output $Y(s)$ is defined as:

$$Y(z) = \frac{\left(1-e^{-(T/\lambda)}\right)z^{-(K+1)}}{\left(1-z^{-1}\right)\left(1-z^{-1}\,e^{-(T/\lambda)}\right)} \tag{14}$$

If the input is a unitary step, the transfer function of the (output/input) is represented as follows:

$$T(z) = \frac{\left(1-e^{-(T/\lambda)}\right)z^{-(K+1)}}{1-e^{-(T/\lambda)}\,z^{-1}} \tag{15}$$

The Dahlin digital controller's transfer function can be expressed subsequently:

$$C_{Dahlin}(z) = \frac{1}{G(z)}\left[\frac{T(z)}{1-T(z)}\right] \tag{16}$$

Where $G(z)$ is the Z-transform of the DC-DC BC transfer function and is computed by the following steps.

$$G(z) = Z\left\{\left(\frac{1-e^{-T_s}}{s}\right)\frac{\frac{u_0}{LC}\left(\frac{L}{R_0(1-d)}s+1\right)}{\left(s^2+\frac{1}{R_0C}s+\frac{(1-d)^2}{LC}\right)}\right\} \tag{17}$$

$$G(z) = \left(1-z^{-1}\right)Z\left\{\frac{1}{s}\cdot\frac{5.333\cdot10^4\,s+2.691\cdot10^7}{s^2+1333\,s+6.728\cdot10^5}\right\} \tag{18}$$

The sampled transfer function of the DC-DC BC system expressed by the equation (19) is obtained by decomposing the preceding formula into simple elements and using the Z-transform properties expressed by the following formula.

$$G(z) = \frac{0.0480\,z^{-1}-0.0480\,z^{-2}}{1-1.9988\,z^{-1}+0.9988\,z^{-2}} \tag{19}$$

Taking the time constant $\lambda = 2\cdot10^{-3}$, the degree operator K = 1, and using formula (16), the transfer function of the Dahlin digital controller is presented by the following equation:

$$C_{Dahlin}(z) = \frac{10^{-3}\left[0.4494\,z^{-4}-0.8993\,z^{-3}+0.4499\,z^{-2}\right]}{\left[0.0479\,z^{-3}-0.0959\,z^{-2}+0.0480\,z^{-1}\right]} \tag{20}$$

VI. Results of Simulation:

To compare the performance of these two digital controllers, discrete FLC and Dahlin using the DC-DC BC's voltage control mode (VCM) methodology, simulation results are given with the system parameters in the Appendix.

Fig. 5, Fig. 6, and Fig. 7 summarize the responses of the error, the duty cycle, and the output voltage of the DC-DC BC controlled by the two digital controllers discrete FLC and Dahlin with critical changes in the voltage reference of 12, 17, 10 and 13 volts at time intervals of [0 0.2](s), [0.2 0.4](s), [0.4 0.6](s) and [0.6 0.8](s). When changing the reference, the Dahlin controller converges faster than the discrete FLC controller.

The DC-DC BC is initially supplied with 10 volts, then given a change in input voltage from 10 to 14, and then 12 volts at t = 0.1 (s) and t = 0.2 (s), respectively. Fig. 8 shows that the output voltage response with the discrete FLC and Dahlin controllers remains unchanged except for a minimal overshoot. Still, the Dahlin overshoot is rapid during the sudden input voltage change.

Finally, the output response of the DC-DC BC for a change in load, with the load resistance changed from 20 Ω to 2 Ω at t = 0.15 (s), was analyzed. The simulation results in Fig. 9 show that both the discrete FLC and Dahlin digital controllers adapt immediately with low overshoot and satisfactory tracking of the reference voltage.

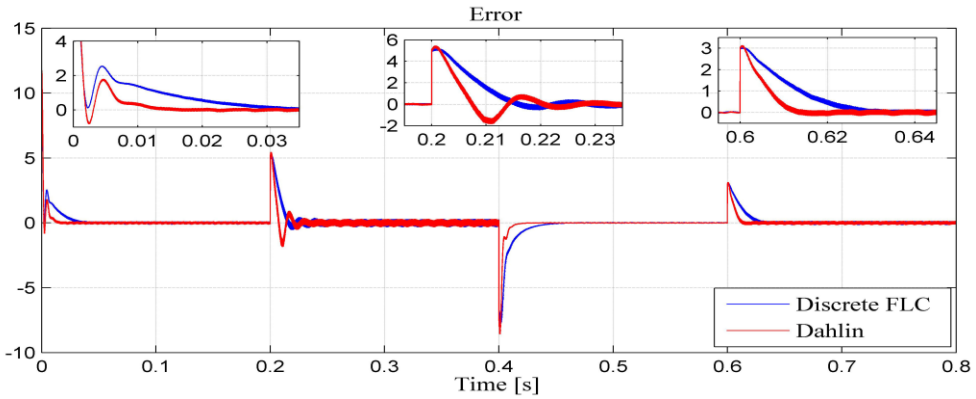

Fig. 5. Error response versus time of the two digital controllers, FLC and Dahlin.

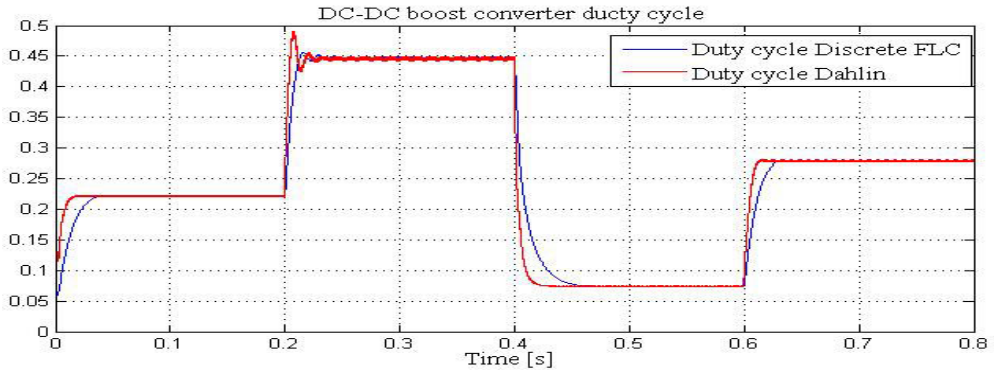

Fig. 6. Duty cycle response versus time of the DC-DC BC with the two digital controllers, FLC and Dahlin, under critical reference voltage change.

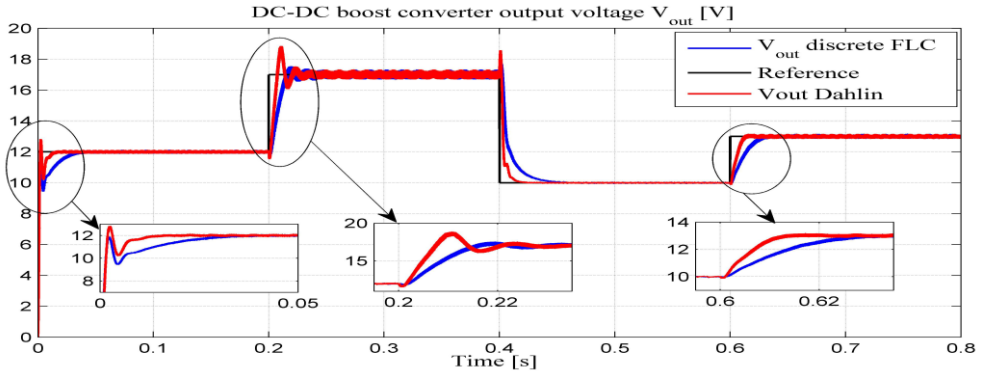

Fig. 7. Output voltage response versus time of the DC-DC BC with the two digital controllers, FLC and Dahlin, under critical reference voltage change.

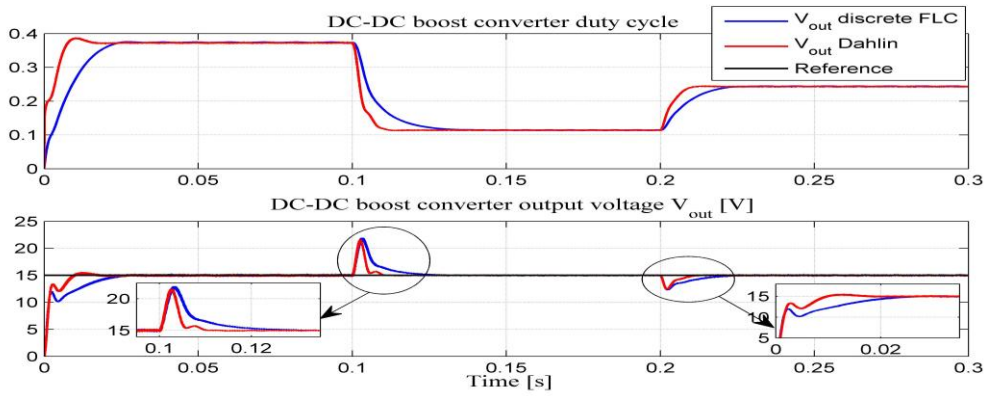

Fig. 8. Output voltage response versus time of the DC-DC BC with the two digital controllers, FLC and Dahlin, under critical input voltage change 14 [V] at 0.1 [s] and 12[V] at 0.2 [s].

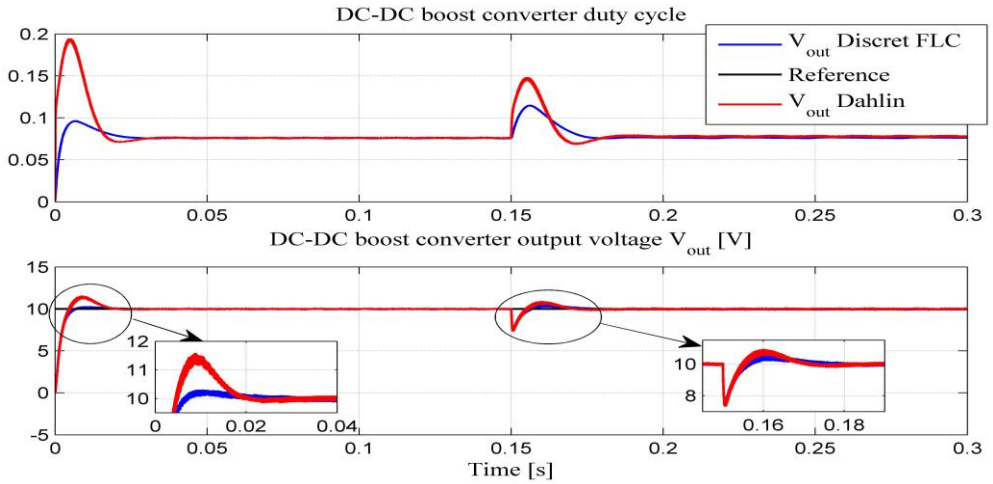

Fig. 9. Output voltage response versus time of the DC-DC BC with the two digital controllers, FLC and Dahlin, under critical load resistance change from 20 [Ω] to 2 [Ω] at 0.15 [s].

TABLE I. SIMULATION PARAMETERS

Parameters	Variables	Values
Inductance	L	$3.716\,(mH)$
Capacitance	C	$100\,(\mu F)$
Load resistance	R_0	$7.5\,(\Omega)$
Switching frequency	F_s	$20\,(Khz)$
Duty cycle	d	0.5
Supply voltage	u_0	$10\,(V)$
Sampling time	T_s	$0.9\,(\mu s)$

VII. CONCLUSION:

In this study, the SSA linearization approach is employed to obtain the mathematical model of the Boost converter. Two discrete digital controllers, discrete FLC and Dahlin, have been created and employed in the voltage control mode (VCM) for continuous conduction mode (CCM). The two digital controllers, discrete FLC and Dahlin, are compared for a sudden change in input voltage amplitude and in load resistance. The Dahlin controller reacts more dynamically, fastly, and robustly to external changes than the discrete FLC controller. Simulation results in MATLAB Sim-Power-Sytems environment confirm the efficacy of suggested control measures.

ACKNOWLEDGMENT

The authors express their gratitude to the organizers and scientific committee of the 2nd International Conference on Electrical Engineering and Renewable Energy Systems (ICEERES'2025), held in Béchar, Algeria, on November 26-27, 2025, for the successful execution of the event and the significance of the presented work.

REFERENCES

[1] G. Eason, B. Noble, and I. N. Sneddon, "On certain integrals of Lipschitz-Hankel type involving products of Bessel functions," Phil. Trans. Roy. Soc. London, vol. A247, pp. 529–551, April 1955.

[2] P. Verma, M. N. Anwar, M. K. Ram, and A. Iqbal, "Internal Model Control Scheme based Voltage and Current Mode Control of DC-DC Boost Converter," *IEEE Access, pp. 110558-110569, 2023, doi: 10.1109/ACCESS.2023.3320272*.

[3] Le Hoai Nam, K. Orikawa and J. -i. Itoh, "DCM control method of boost converter based on conventional CCM control," *2014 International Power Electronics Conference (IPEC-Hiroshima 2014 - ECCE ASIA)*, Hiroshima, Japan, 2014, pp. 3659-3666, doi: 10.1109/IPEC.2014.6870024.

[4] A. Marahatta, Y. Rajbhandari, A. Shrestha, S. Phuyal, A. Thapa, and P. Korba, "Model predictive control of DC/DC boost converter with reinforcement learning," *Heliyon*, vol. 8, Issue 11, November 2022, https://doi.org/10.1016/j.heliyon.2022.e1141

[5] C.-S. Lee, M. Gendensuren, B. Dansran, B.-C. Ahn, and S.-G. Choi, "Integrated 0.35-µm CMOS Control Circuits for High-Performance Voltage Mode DC–DC Boost Converter," *Electronics*, vol. 12, N°: 1, p. 133, 2022. https://doi.org/10.3390/electronics12010133.

[6] F. Tahri, A. Tahri, A. Allali, and S. Flazi, "The digital self-tuning control of step a down DC-DC converter," *Acta Polytechnica Hungarica*, vol. 9, N° 6, pp. 49-64, 2012.

[7] [6] H. Ji, F. Xie, Y. Chen, and B. Zhang, "Small-step discretization method for modeling and stability analysis of cascaded DC–DC converters with considering different switching frequencies," *IEEE Transactions on Power Electronics*, vol. 37, no. 8, pp. 8855-8872, Aug. 2022, doi: 10.1109/TPEL.2022.3155740.

[8] A. Koduah and F. B. Effah, "Fuzzy-Logic-Controlled Hybrid Active Filter for Matrix Converter Input Current Harmonics," *Energies*, vol. 15, n° 20, p. 7640, 2022. https://doi.org/10.3390/en15207640

[9] S. Rajendran, V. Thangavel, N. Krishnan, and N. Prabaharan, "DC link voltage enhancement in DC microgrid using PV based high gain converter with cascaded fuzzy logic controller," *Energies*, vol. 16, n° 9, p. 3928, 2023. https://doi.org/10.3390/en16093928

[10] G. Tahri, Z. A. Foitih, and A. Tahri, "Fuzzy logic control of active and reactive power for a grid-connected photovoltaic system using a three-level neutral-point-clamped inverter," *International Journal of Power Electronics and Drive Systems*, vol. 12, N° 1, March 2021, pp. 453-462,. http://doi.org/10.11591/ijpeds.v12.i1.pp453-462

[11] G. Tahri, F. Tahri, and A. Tahri, "Fractional order PID controller design of a DC-DC multilevel boost converter using the Nelder-Mead optimization," *International Journal of Power Electronics and Drive Systems (IJPEDS)*, vol. Vol 15, Nº 4 December 2024. pp. 2409-2421, DOI: 10.11591/ijpeds.v15.i4.pp2409-2421.

[12] S. Walz, R. Lazar, G. Buticchi, and M. Liserre, "Dahlin-based fast and robust current control of a PMSM in case of low carrier ratio," *in IEEE Access, vol. 7, pp. 102199-102208, 2019, doi: 10.1109/ACCESS.2019.2927402.*